

Revisión / Review

Deep Lichen-Net: Deep learning based automatic classification and segmentation of Lichens in Western Ghats, India

[Deep Lichen-Net: Clasificación y segmentación automática de líquenes en los Ghats occidentales de India basada en aprendizaje profundo]

Amsaveni Govindasamy¹, Ponmurugan Ponnusamy², Punietha Prabhu¹ & S. M. Ramesh⁴

¹Department of Biotechnology, K S Rangasamy College of Technology, Tiruchengode Namakkal, Tamil Nadu, India

²Department of Botany, Bharathiar University, Coimbatore, Tamil Nadu, India

³Department of Electronics and Communication Engineering, KPR Institute of Engineering and Technology, Coimbatore, India

Reviewed by:

Leda Guzman
Universidad Católica de Valparaíso
Chile

Alina Freire
Universidad Tecnica de Cotopaxi
Ecuador

Correspondence:

Amsaveni GOVINDASAMY
Amsaveni345@outlook.com

Section Ethnobotany

Received: 29 May 2024

Accepted: 20 August 2024

Accepted corrected: 1 December 2024

Published: 30 May 2025

Citation:

Govindasamy A, Ponnusamy P, Prabhu P, Ramesh SM.
Deep Lichen-Net: Deep learning based automatic
classification and segmentation of Lichens in
Western Ghats, India

Bol Latinoam Caribe Plant Med Aromat

24 (3): 328 - 344 (2025)

<https://doi.org/10.37360/blacpma.25.24.3.24>

Abstract: Lichens are a symbiotic association between fungal and photoautotrophic algal partners that exhibit vast diversity in India with around 2,300 species recorded. In this research, a novel deep learning method known as LichenNet is proposed for the classification of lichens gathered from Western Ghats, India. Initially, the gathered images are denoised with Bright contrast dynamic histogram equalization (BCDC) filter to enhance the image quality and these are augmented to increase the images in the dataset. The Region of Interest (ROI) method is applied for generating the image patches by dividing the non-overlapping segments. The Dilated LinkNet is integrated with local and global sampling to extract the fine features while the Pelican Optimization (PeO) algorithm selects the best features for classification. The proposed LichenNet achieves the classification accuracy of 99.26%. The proposed LichenNet progresses the overall accuracy of 2.19%, 4.29%, and 14.36% for XGBoost, SIFT and CNN respectively.

Keywords: Lichen species; Deep learning; Patch extraction local and global features; Pelican optimization algorithm; Dilated LinkNet

Resumen: Los líquenes son una asociación simbiótica entre hongos y algas fotoautótrofas que exhiben una gran diversidad en India, con alrededor de 2.300 especies registradas. En esta investigación se propone un nuevo método de aprendizaje profundo conocido como LichenNet para la clasificación de líquenes recolectados en los ghats occidentales de India. Inicialmente, se reduce el ruido en las imágenes recolectadas con un filtro de eualización de histograma dinámico de contraste brillante (BCDC) para mejorar la calidad de la imagen y se aumentan para incrementar la cantidad de imágenes en el conjunto de datos. Se aplica el método de Región de Interés (ROI) para generar parches de imagen dividiendo los segmentos no superpuestos. El Dilated LinkNet se integra con muestreo local y global para extraer características finas, mientras que el algoritmo de Optimización Pelicano (PeO) selecciona las mejores características para la clasificación. El LichenNet propuesto alcanza una precisión de clasificación del 99.26%. Además, el LichenNet propuesto mejora la precisión general en un 2.19%, 4.29% y 14.36% para XGBoost, SIFT y CNN respectivamente.

Palabras clave: Especies de líquenes; Aprendizaje profundo; Extracción de parches; Características locales y globales; Algoritmo de optimización pelicano.

INTRODUCTION

Lichen is a symbiotic organism that consists of two or more fungi and a photosynthetic partner, typically algae or cyanobacteria (Spribille *et al.*, 2016). A wide variety of environments rely on them for soil creation, nutrient cycling, and biodiversity (Devaprakash *et al.*, 2024; Jung *et al.*, 2024). It is crucial to accurately identify lichen species for ecological studies, conservation initiatives, and environmental health. Around 20,000 different types of lichens are readily found all over the world, and India is inhabited to over 2300 species (Hrdina & Romportl, 2024). Lichens are vital components of many ecosystems and serve to monitor environmental conditions. Furthermore, these organisms are identified using microscopy techniques, a technique that requires expertise and is time-consuming to observe the physical traits (Lie *et al.*, 2009). The colors of lichens range from bright yellows and greens to deep browns and grays. Pigments like anthocyanins, carotenoids, and chlorophyll can provide indicators about the identity of some species (Ovstedal & Smith, 2001). There are certain characteristics that are essential to adequately characterize a species. There are morphological traits, which provide physical descriptions; genetic markers, which reveal inheritance information; ecological preferences, which indicate the species' preferences for particular habitats and environments; and geographical distribution, which describes the species' natural habitats. These characteristics are specifically assessed using microscopy because this method provides unique and critical details that cannot be accurately captured or replicated by any other evaluation technique. Therefore, it is essential to use microscopy for these evaluations to ensure the precision and reliability of the observations. The identification of lichen species can be further improved by considering their ecological preferences and geographic distribution, since some species may only be found in particular areas (Kapoor *et al.*, 2022; Haridas *et al.*, 2023). This tool could become very important in the study area, the Indian Western Ghats, which is a biodiversity hotspot to many plant and animal species, including many lichen species.

Nowadays, machine learning (ML) (Vinayaka & Krishnamurthy, 2010) and deep learning (DL) (Surendiran *et al.*, 2022) techniques are significant procedures for diagnosing diverse ailments. Automated systems are created to identify and

categorize different species of lichen based on images using deep learning networks (Dinesh *et al.*, 2019). The development of robust deep learning models for lichen identification holds promise for citizen science initiatives, where enthusiasts and non-experts can contribute to biodiversity monitoring efforts by simply capturing and uploading images of lichens for automated species identification (Guedes *et al.*, 2022; Dakshina *et al.*, 2023). Identifying lichen species traditionally relies on labor-intensive morphological and chemical analyses, which are time-consuming and require expertise. DL models are adapted to the specific task of lichen identification will be employed to mitigate the need for vast amounts of labelled data and reduce training time (Jozdani *et al.*, 2021; Prasanth & Muthukumaran, 2023). This study pays to the growing field of computer vision in ecology and biodiversity studies, demonstrating the potential of DL to streamline taxonomic identification processes and enhance our understanding of lichen diversity and distribution patterns. The key contributions of this paper are plotted as follows:

- This paper introduces a novel Deep LichenNet for the identification of lichen main categories, aiming to develop an efficient and accurate system for species classification.
- Lichen images are collected from the Western Ghats, and Generative Adversarial Network (GAN) architecture is used for image augmentation at different angles to expand the dataset, with noisy artifacts removed for training purposes.
- The lichen image patches are generated using RoI by dividing the images into non-overlapping segments, followed by local feature extraction from each patch.
- The Dilated LinkNet is integrated with local and global sampling modules to enhance feature extraction process for classifying various lichen species.
- These features are then input into the PeO algorithm to select the most relevant ones for classifying lichen

taxa into fruticose, crustose, and foliose categories.

Background study

DL-based convolutional neural networks (CNNs) was established an extraordinary effectiveness in a variety of image categorization tasks because they learn from raw images automatically and extract characteristics automatically (Jozdani *et al.*, 2021). In the Western Ghats, India, LinkNet was trained on large image datasets for lichen classification, which allows recognition and differentiation of Crustose (Peng *et al.*, 2020) and foliicolous species of lichen (Rajaprabu & Ponmurugan, 2022; Subbaiyan *et al.*, 2023). To create a variety of training samples, these models use data augmentation, which rotates and scales the source images. It is especially useful since lichens can appear differently depending on the environment. Moreover, hyperspectral and multispectral imaging data can be combined to enhance classification performance even further by providing rich spectral information that is frequently indicative of several lichen species (Granlund *et al.*, 2018). Through the application of deep learning, conservation and research efforts in the Western Ghats, India, could be enhanced by streamlining the classification process and improving monitoring reliability (Erlandsson *et al.*, 2022).

Lichens in the Western Ghats are classified by a deep learning based LinkNet, an innovative approach to biodiversity research and conservation (Malik *et al.*, 2022). The LinkNet architecture was used to identify lichen species in the Western Ghats for efficient classification of fruticose, crustose, and foliose categories (Vinayaka *et al.*, 2016). LinkNet's encoder-decoder architecture and residual connection technology enable the feature extraction process with high precision for lichen image classification into different categories. Lichens are particularly useful for managing their intricate and varied visual properties (Li *et al.*, 2021; Wang & Jia, 2024). LinkNet is used with the large collection of images of Western Ghats lichen to distinguish between several species based on their distinctive visual patterns and textures, where the use of hyperspectral and multispectral imaging data is another method that enhancing the accurateness and robustness of the model (Mishra *et al.*, 2021). In the ecologically substantial region, LinkNet's lichen classification streamlines the identification process while offering a scalable solution for biodiversity

monitoring (Guedes *et al.*, 2022).

Literature Review

Many researchers have published studies identifying lichen types using digital image processing and classification methods in the past. Recent advances in ML and DL approaches can be found in a variety of literature works.

Sandino *et al.* (2023), conducted validation in this field by obtaining ground and aerial image at ASPA-135, East Antarctica. The data collection stage included employing a data fusion method to merge Hyperspectral Imaging (HSI) and Multispectral Imaging (MSI) data, resulting in the acquisition of geo-referenced HSI images. XGBoost was used in the model training process, and four various combinations were explored to find the best match for the data. The fallouts of the research demonstrate that moss and lichens were successfully identified with an average accuracy of 95%.

Richardson *et al.* (2023), evaluated ML models based on their capability to identify lichen coverage in Sentinel-2 imagery in Quebec and Labrador, Canada. Lichen coverage maps, at 10-meter resolution, were created from 20 drone scans conducted between July 2019 and 2022, serving as the training data. The dense neural network attained the highest accuracy, with a mean absolute error of 5.2%, outperforming the convolutional neural network (5.3% error) and the random forest model (5.5% error).

Lovitt *et al.* (2022), assessed the efficacy of a DPC approach in quantifying the ground cover percentage of glistening lichens. These lichens serve as a crucial food source for caribou during the Autumn and Winter seasons, especially when alternative food supplies are scarce. The methodology utilized licensed software. However, contrasting this licensed procedure, the Lichen Convolutional Neural Network (LiCNN) presents a more dependable and efficient solution. LiCNN, is a classification model effectively overcomes the constraints of traditional ground-truth data gathering approaches without requiring particular software.

Presta *et al.* (2022), employed a ML methodology centered on patch classification to categorize lichen taxa based on images. Three distinct approaches for patch descriptor extraction: (i) manually crafted descriptors employing traditional feature extraction algorithms, (ii) CNN utilized as

feature extractors, and (iii) scattering methods that integrate nonlinear operators and wavelet convolutions. This model attained the highest accuracy of 0.89 by employing dense SIFT by leveraging on a lichen dataset.

Galanty *et al.* (2021), introduced a classification tool for identifying *Cladonia* lichens based on deep convolutional neural networks. The study utilized eleven species of *Cladonia* for both training and testing the network, compiling a dataset of 1164 images sourced from numerous websites. The accuracy of the trained system attains 60.94% demonstrates promising performance for this nascent automatic categorization of lichen species.

Preethaa *et al.* (2021), had discussed the growth of lichen elements on the facades of buildings within intelligent urban areas. After this discourse, it is evident that the Resnet-152 demonstrates proficiency in extracting color features from lichen images. The Unmanned Ariel Vehicle functions autonomously to gather these images from building surfaces. The extracted features undergo processing through the convolutional and max-pooling layers of the Resnet architecture. Subsequently, the input image was vectorized and categorized on contamination levels.

Idrees *et al.* (2021), employed digitalized hematoxylin and eosin microscope slides to detect and measure mono-nuclear cells and granulocytes in inflammatory penetrates using a ML based artificial neural network. To aid educational endeavours, 24 regions of interest were retrieved from cases of oral lichen planus (OLP), subsequently validated against a retrospective cohort comprising 130 cases. This study identified a threshold on the quantity of mono-nuclear cells that effectively distinguished OLP from other lichenoid conditions by achieving a 94.62% accuracy rate.

Rehush *et al.* (2018), examined the probable of close-range terrestrial laser scanning (TLS) for the semi-automated detection of various Tree-Related Microstructures (TreMs) within dense TLS point clouds employing deep learning. Multiple deep learning networks were trained with rasterized Multiview Orthographic Projections (MVOPs) incorporating front, top, and side views of the 3D local point surroundings, to classify TreMs. The

$$R = \begin{cases} o * \alpha & 0 \leq \alpha < u \\ p * (\alpha - u) + i & u \leq \alpha < v \\ q * (\alpha - v) + j & v \leq \alpha < G - 1 \end{cases} \quad (1)$$

Random Forest (RF) model achieved a 70.0% overall accuracy confirming the efficacy of leveraging local geometric features for classifying six TreM groups.

From these existing techniques, automatic classification and segmentation of lichens in the Western Ghats could be the limited availability of high-quality training data. The existing models may struggle to generalize well to unseen lichen specimens or environmental conditions, leading to reduced classification and segmentation accuracy. Moreover, variations in lighting conditions, image quality, and background clutter in field-collected lichen images can introduce challenges for automated classification and segmentation algorithms. This research work distinguishes itself by proposing the novel LichenNet for lichen classification, utilizing a LinkNet dilated convolutional layers instead of standard convolutional layers for efficient feature extraction. Moreover, we utilized local and global sampling modules to enhance feature extraction process in LinkNet architecture. Additionally, it employs the PeO algorithm for optimal feature selection, aiming to improve classification accuracy. The combination of these methods presents a unique approach in the domain.

PROPOSED METHODOLOGY

This section presents a novel Deep LichenNet was introduced for the classification of lichens from the gathered lichen dataset. Figure No. 1 shows the general procedure of the proposed method for lichen classification.

Image denoising via BCDC filter

The different lichen images were collected from the Western Ghats and the histograms equalization are employed to enhance the visibility of details in the images by rearranging intensity values, ensuring the full range of intensity values is utilized. Bright contrast dynamic histogram equalization (BCDC) filter employed to boost the contrast of an image by dynamically adjusting its histogram. The BCDC filter involve updating the pixel value of the processed pixel by calculating weights and considering nearby pixel values. The equation (1) illustrates the transformation function utilized to achieve contrast stretching for each pixel in the image.

Where R is the transformed output pixel value after applying the contrast stretching function, α is the input pixel value in the original image, and G indicates the maximum possible value for the pixel intensity. o, p, q represents the constants that determine the slope of the transformation function in different segments. u, v defines the threshold values that define

the breakpoints between different linear segments in the transformation function, and i, j are the offset values added to the scaled pixel values in the second and third segments, respectively. These offsets adjust the output pixel values to achieve the desired contrast stretching effect.

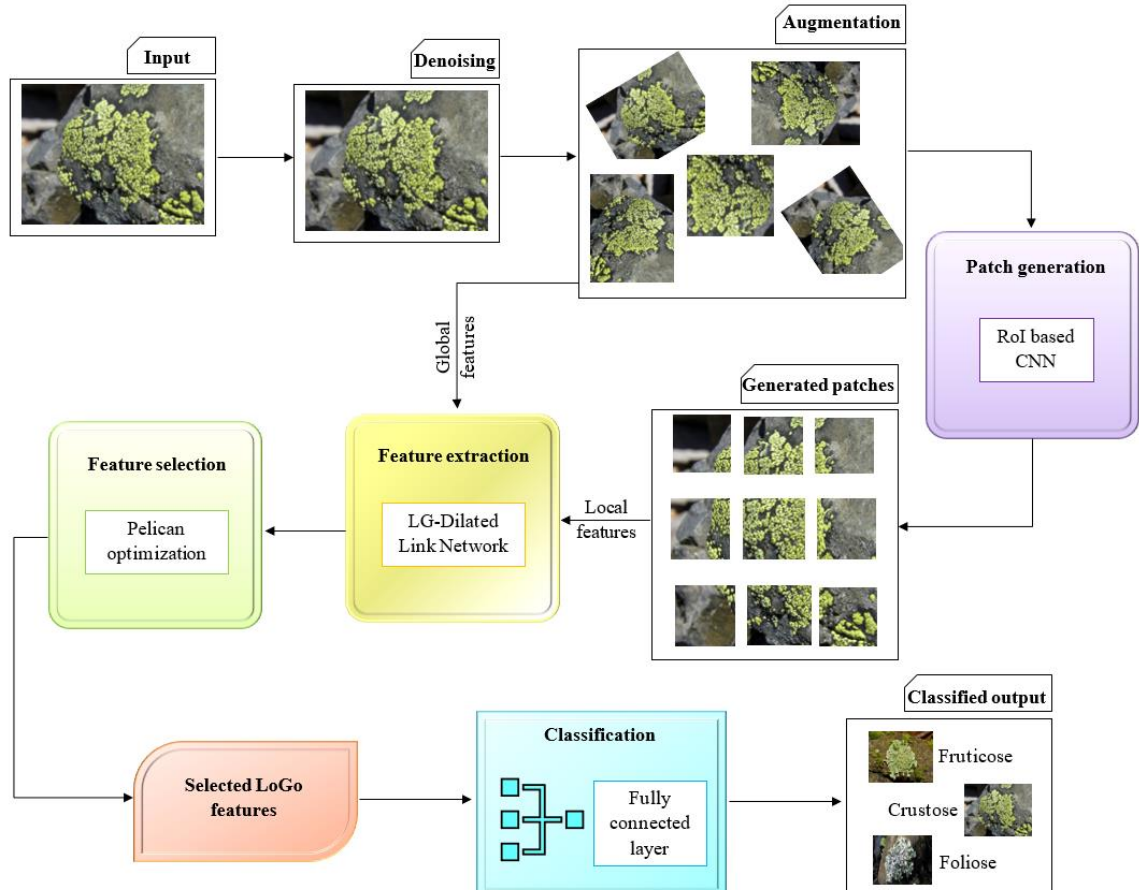


Figure No. 1
Schematic depiction of the proposed Lichen classification model

To improve an image while preserving its features, BCDC filter manages standard HE functions. BCDC filter divides the input histogram into multiple sub-histograms until ensuring that none of the new sub-histograms contains a dominant section. Smoothing towards the data in the histogram is achieved using a one-dimensional Gaussian filter. Equation (2) delineates the parameters of the Gaussian filter.

$$f(G) = \exp\left(-\frac{G^2}{2\sigma^2}\right) \quad (2)$$

From equation (2) G is a vector with relation to the kernel's axis. σ^2 be the standard deviation function. The following equations (3) offer the set of variables for the dynamic equalization method.

$$G_{\mathcal{R}} = m_n - s_n \quad (3)$$

From the equation (3), $G_{\mathcal{R}}$ represent the total amount of pixels in the segment is used to determine spanning. $m_n - s_n$ are the two intensities at their most and least values from the n^{th} input sub-histogram.

$$Start_n = \sum_{y=1}^{x-1} Range_\varepsilon + 1 \quad (4)$$

$$Stop_n = \sum_{y=1}^x Range_\varepsilon \quad (5)$$

Equation (4) and (5) depict the computation of the n^{th} output sub-histogram. It is necessary to acquire remapped values to ensure equilibrium in each sub-histogram. Equation (6) signifies the outcomes of the sub-histogram.

$$\rho(y) = a_n + Range_x \sum_y a_n \frac{v(y)}{\alpha_y} \quad (6)$$

From the above equation (6), $\rho(y)$ represent the distinct level of intensity and a_n means the total number of pixels. The complete range of variable levels is distributed among sub-histograms according to the dynamic range of the input image of histogram data. This distribution of the contrast stretching range ensures effective enhancement of contrast in each region of the entire image, preventing small details in the input image from becoming dominant and fading away. Then, the distinct transformation function, based on the conventional method is generated for each sub-histogram, and the processed images are accordingly transformed into the output image.

$$\min_G \max_D \mathbb{V}(G, D) = \mathbb{E}_{x \sim p_{data}(x)} [\log D(x)] + \mathbb{E}_{z \sim p_z(z)} [\log(1 - D(G(z)))] \quad (7)$$

Where $p_{data}(x)$ defines the true data distribution, $p_z(z)$ defines preceding distribution of the input noise, \mathbb{E} signifies the expectation over the respective distributions.

ROI based Patch generation

The R-CNN network comprises three essential layers: the backbone, RPN, and ROI. Employing convolution techniques, conceptual features are extracted from input images. The convolution feature maps act as the starting point for both refining proposal results and

$$RPN_{loss} = A_{loss} + \mathbb{H}_{loss} = \sum_{i=1} A_{loss}(fm_i) + \mathbb{H}_{loss}(fm_i) \quad (8)$$

Where fm_i signifies the feature-maps from the i^{th} scale. The ROI layer takes as input the feature maps resulting from the backbone and the RPN proposal. This yields an array of potential candidate boxes likely to contain the desired object. IoU is leveraged to

GAN based data augmentation

GAN structure is DL network that includes two components: generator and discriminator. The framework employs small batch training for both the discriminator D and generator G, thereby amplifying learning consistency and generalization efficiency. G provides random noise z as input and produces a synthetic image x' . Mathematically, the generator function is denoted as $x' = G(z, \vartheta_g)$. Where z is the random noise vector sampled from a prior distribution, ϑ_g signifies the parameters of the generator. The discriminator D gets an image as input and output with a prospect signifying whether the input is real or synthetic. Mathematically, the discriminator function can be denoted as $D(x, \vartheta_d)$.

During training, the G and D are trained simultaneously in a minimax game scenario. G receives two inputs: the class label y and a random noise vector z , drawn from a Gaussian distribution. These inputs are separated and then utilized to generate new attack samples, denoted as $G(z)$, which are produced through the training process. The objective is to minimize the following value function:

acquiring segmentation in the ROI network, as well as providing foreground-containing proposals in the RPN. The ResNet50 framework is utilized in this process, generating a variation of feature-maps of various sizes through continuous stride operations. At the RPN phase, three types of anchors with diverse length-to-width proportions are accessible. Rather than utilizing multiscale anchors, a scale-specific map is generated with the foreground detection. The loss function of the RPN encompasses of regression and box classification losses.

refine boundary boxes for increased accuracy. Subsequently, following corrections made by the ROI phase, improved feature-maps are obtained through RoIAlign and given to the mask-layer for object segmentation. Rather than employing a fully connected network, a convolutional network is

utilized for classification and regression tasks. The

$$RoI_{loss} = A_{loss} + H_{loss} + S_{loss} \tag{9}$$

Equations (8) and (9) demonstrate the intricacy of the RCNN's loss function at both the RPN and RoI layers. The loss function at the ROI layer encompasses three components classification loss A_{loss} , Regression loss H_{loss} and segmentation loss S_{loss} , indicating its complexity. The RoIAlign process will employ this technique to merge feature maps

$$S_{loss} = \alpha CE_{loss} + \beta B_{loss} + \gamma C_{loss} \tag{10}$$

Where CE_{loss} signifies the loss of cross-entropy, B_{loss} means the boundary loss, C_{loss} signifies the networks' cutloss, and $\alpha = 1, \beta = 1.5, \text{ and } \gamma = 1.5$ are the weights for aforesaid losses. The human eye tends to inaccurately estimate the cross-entropy loss (CE_{loss}) maintained in image segmentation for multiple isolated pixels in classification problems, as expressed in equation (10).

LG-Dilated LinkNet

In this section, LG-Dilated LinkNet encompasses with Dilated convolution, local and global sampling to extract the efficient features. The LinkNet architecture comprises a sequence of encoder and decoder blocks that break down the image and reconstruct with few convolutional layers. Moreover, this architecture encompasses with sampling mechanisms for extracting the local and global (LoGo) features from

$$\hat{s}_i = s_i + (s_i - 1) \times (d_i - 1) = d_i \times (s_i - 1) + 1 \tag{11}$$

Let z represent the convolution in f^{th} layer ($f = 1, 2, \dots, F$), and K_Q demonstrate the filter

$$\begin{cases} K_{Qf} = z_{f-1} \times K_{Qf} + s_{1f-1} \widehat{z}_{f-1} \\ K_Q = 1 \end{cases} \tag{12}$$

The LinkNet architecture differs significantly from neural architectures for pixel-wise operation.

cumulative loss of the ROI layer is determined by,

containing various scales into a unified scale. Additionally, the segmentation layer is responsible for segmenting the RoI. To generate a dense prediction distinct from the earlier classification and regression layers, R-CNN utilizes a convolutional network along with a segmentation loss function.

the patches and denoised images. LinkNet operates as a semantic segmentation network to retain a good deal of the spatial features in the image. The architecture of Deep learning based LinkNet for Lichen classification is shown Figure No. 2. The technique entails joining the encoder module's shallow feature map directly to the similarly sized decoder module. By utilizing the precise position data from the shallow layer, this method reduces the need for extraneous calculations and parameters, which speeds up computation without sacrificing precision.

The dilated rate d_i in dilated convolutional layer signifies sub-sampling the feature maps by a factor of $d_i - 1$ or inserting d_i zeros among the filter weights. Equation (11) gives the size of the resultant d_i -dilated convolutional filter for a 1×1 dilated convolutional filter size $s_i \times s_i$, respectively.

dimension of every dilated layer at d_i and is expressed in below equation (12).

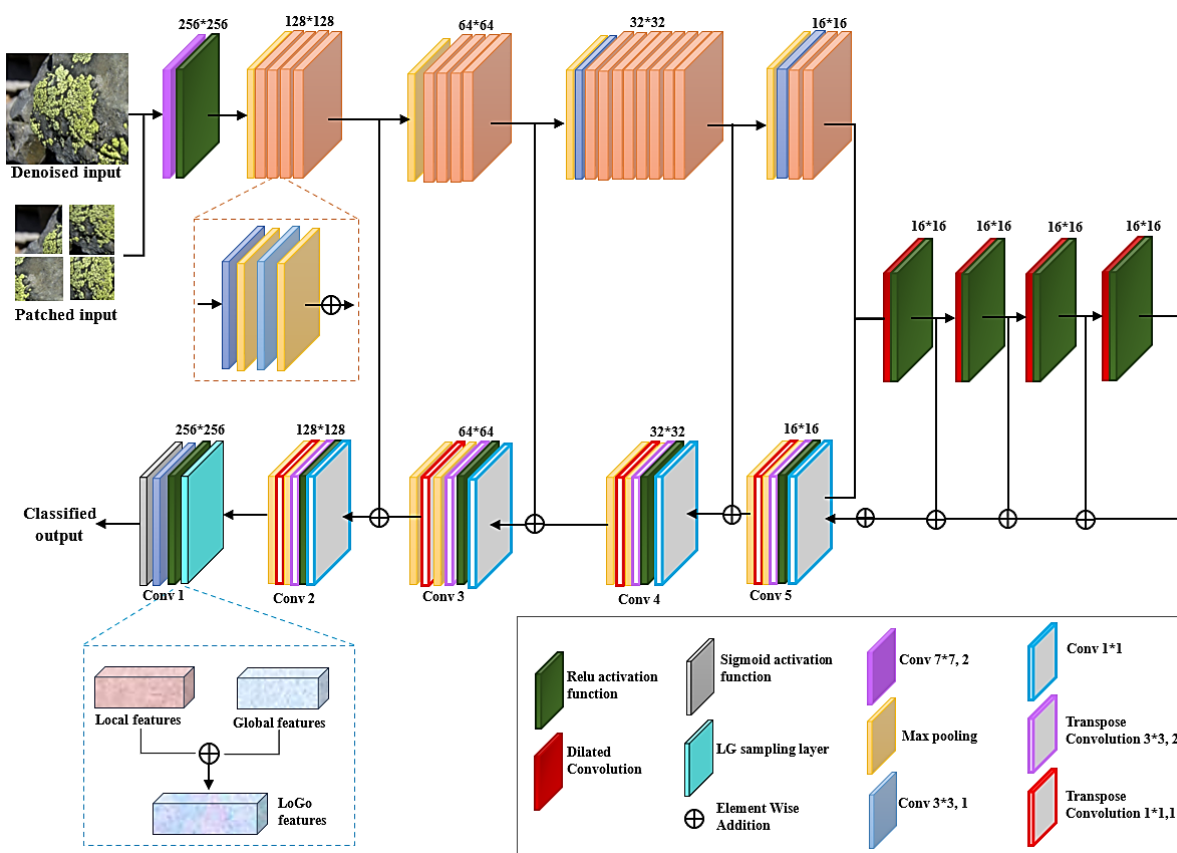


Figure No. 2
Architecture of Deep learning based LinkNet for Lichen classification

Its uniqueness lies in the connection between the encoder and decoder. Spatial information loss during decoding, and recovering it from the encoder's output is challenging. In LinkNet, the encoder and decoder are linked through non-trainable pooling indices. This link recovers spatial information lost during encoding, crucial during the decoder's up sampling. In this architecture, the decoder uses fewer parameters, sharing knowledge acquired by the encoder.

Local sampling

The main objective of this algorithm is to extract particular local features from patch images input. The upscaled photos are guaranteed to preserve the finer details of the original images since the generator is trained on these local features. During image upscaling, local sampling is essential for learning and improving the details lost in the low-resolution input image. By prioritizing local features during training,

the generator preserves and enhances these characteristics while upscaling images.

Global sampling

Denoised images are analyzed by extracting their global characteristics and looking at their composition and structure. As a result, the upscaled images display a global structure similar to the input images while also capturing local details. Global structures are derived by progressively downsampling the original images using convolutional layers until the result is the sum of global feature channels. The local function map f_l at measure u with width $l_x \times w_y \times c_z$ and the global function f_g , with length $1 \times 1 \times f_g$. During channel pairing, the global structures are familiar using a 1×1 unit with accessible weights. The limit values for the phase are as follows: filter dimension 1×1 , the quantity of frequencies f_g , and the total output networks S_f , respectively. The fused feature patches f_g and f_l with the equal size are merged and

the evaluate the patches are derived in equation (13).

$$S_{res} = \mathcal{F}_{patch}(f_a, f_i) \quad (13)$$

From the above equation, S_{res} signifies the super resolution image, and \mathcal{F}_{patch} represents the fused patches of the f_a and f_i respectively.

Pelican Optimization algorithm

The PeO algorithm is employed for feature selection, reducing the number of features in the images and selecting a subset to enhance classification accuracy. Inspired by the behavior and lifestyle of pelicans, the PeO algorithm selects the best features from the preceding network. In this algorithm, the number of pelicans signifies the retrieved features from LinkNet. The optimal features are symbolized by the pelican with the highest fitness after catching prey, while

$$z_{i,j}^{s1} = \begin{cases} z_{i,j} + rand \times (p_j - I_r \times z_{i,j}); & F_p < F_i \\ z_{i,j} + rand \times (z_{i,j} - p_j); & else \end{cases} \quad (14)$$

In the equation (14), I_r represents a random number selected between 1 and 2, p_j denotes the target's location in the j th dimension, F_p stands for its objective function, and $z_{i,j}^{s1}$ represents the new position of the i th pelican in the j th dimension during stage 1. The parameter I_r , which can take on the value of either 1 or 2 arbitrarily, determines the degree of displacement. When I_r reaches 2, members may

$$Z_i = \begin{cases} Z_i^{s1}; & F_i^{s1} < F_i \\ Z_i; & else \end{cases} \quad (15)$$

where S_i^{s1} is the new position of the i th pelican and F_i^{s1} is its objective function for stage 1. The Pelican Optimization (PeO) Algorithm works by representing lichen features (such as color, texture, and shape descriptors) as feature sets. Initialize a population of pelicans with random positions corresponding to subsets of these features. The fitness function, typically based on classification accuracy, guides optimization by evaluating each subset. Through iterative updates, pelicans adjust their positions, simulating hunting strategies to find the optimal feature subset that maximizes classification

redundant features correspond to pelicans with the lowest fitness. The PeO algorithm uses two primary hunting tactics: moving towards the prey to generate features and skimming the water's surface to select features.

Stage 1: Moving towards Prey

During the early phase of the hunt, pelicans locate and approach their target. By modeling this technique, the search space can effectively explore different regions. In the Pelican Optimization (PO) method, the prey's position is arbitrarily selected inside the search space, a fundamental aspect of the approach. Equation (14) simulates the pelican's empirical method for identifying its prey.

venture into unexplored areas. Consequently, I_r significantly influences the PeO algorithm's ability to thoroughly explore and accurately scan the search space. If the pelican's new position fallouts in an enhancement in the objective function value, it is accepted by the PeO algorithm. This process is resulting in equation (15).

performance. The final output is the subset of features that offers the best classification accuracy for lichen species identification.

Stage 2: Winging on the Water Surface

In the second stage, pelicans propel fish above the water's surface using their wings before gathering them into their neck pouches. This strategy is employed by pelicans in targeted areas to enhance fish capture. To optimize outcomes, considerations must be made for factors influencing pelican posture. The predatory behavior of pelicans is quantitatively simulated using equation (16).

$$z_i^{s2} = z_{i,j} + n \times \left[1 - \frac{t}{T}\right] \times [2 \times rand - 1] \times z_{i,j} \tag{16}$$







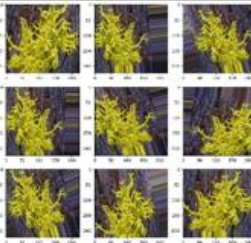
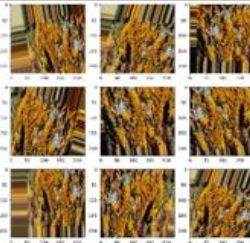
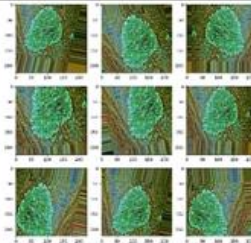
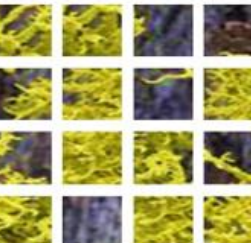

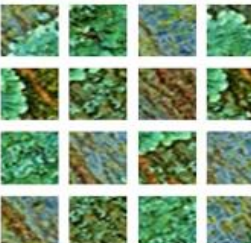



	Input image-1	Input image-2	Input image-3
Input			
Denoising			
Augmentation			
Patch generation			
Feature extraction			
Classified output	Fruticose	Crustose	Foliose

Figure No. 3
Experimental results of the proposed model for Lichen classification

In the equation (16), where n represents a constant set at 0.2, $n \times \left[1 - \frac{t}{T}\right]$ denotes the neighborhood radius of $z_{i,j}$, with tt being the iteration timer and T representing the maximum number of iterations. Furthermore, z_i^{s2} stands for the anticipated new position of the i th pelican in the j th dimension during stage 2. Initially, a larger area surrounding each

$$Z_i = \begin{cases} Z_i^{s2}; F_i^{s2} < F_i \\ Z_i; \text{else} \end{cases} \quad (17)$$

In stage 2, F_i^{s2} represents the anticipated objective function, while S_i^{s2} denotes the new location of the i th pelican. Randomly chosen features are incorporated after multiplying the inputs by the feature vectors. Subsequently, the PeO algorithm undergoes updates influenced by the Moving and Winging operations' features. This refined PeO algorithm can be placed within a fully connected (FC) layer to enhance classification. This approach is commonly employed to identify crucial traits and eliminate those irrelevant or redundant to lichen type classification.

RESULTS AND DISCUSSION

This section used Matlab-2020b to implement the experimental results and assess the efficacy of the proposed Deep LichenNet. In this work, we have collected different lichen images from the Western ghats are the input to the proposed LichenNet for detecting the lichen categories. The Western Ghats are a mountain range located along the western coast of India. The gathered species extend from the state of Gujarat in the north, running through Maharashtra, Goa, Karnataka, and Kerala, ending in Tamil Nadu in the south. This biodiversity hotspot is recognized for its rich variety of flora and fauna. The test sample was evaluated through the use of recall, precision, F1 score, accuracy, and specificity. The comparison provides a detailed description and analysis of the

$$\text{Accuracy} = \frac{TP+TN}{N} \quad (18)$$

$$\text{Precision} = \frac{TP}{TP+FN} \quad (19)$$

$$\text{Specificity} = \frac{TN}{TN+FP} \quad (20)$$

$$\text{Sensitivity} = \frac{TP}{FN+TP} \quad (21)$$

member is considered in the first iteration due to the higher value of this coefficient. As the replication process proceeds, the coefficients $n \times \left[1 - \frac{t}{T}\right]$ for each member decrease, leading to smaller neighborhood radii. Equation (17), subject to efficient modification, also governs the calculation of a new pelican position at this stage.

total accuracy rate besides the competence of the proposed Deep LichenNet. Additionally, the proposed deep learning model is contrasted with traditional deep learning models to prove the efficiency in the classification.

The Figure No. 3 shown the portrays the fallouts of proposed Deep LichenNet with the sample images gathered from Western Ghats. The gathered images are collected and pre-processed using the combination of filtering techniques to remove the noisy artefacts and improve the image quality is presented in row-1. To increase the training dataset different augmentation techniques are used in different angles with the GAN structure is displayed in row-3. Afterwards, these images are fed into the patch generation phase for generating different patches is shown in row-4. The features are retrieved from the generated image patches to recognize different lichen types such as fruticose, crustose and foliose.

Performance scrutiny

The effectiveness of the proposed LichenNet was evaluated with the network metrics viz., F1-score (f1), precision (pre), sensitivity (sen), accuracy (acc), and specificity (spe). The data is splitted into two subsets: 80% for training and 20% for testing. The subsequent metrics are employed to estimate the competence of the proposed system

$$F1\ score = \frac{2 \times TP}{(2 \times TP + FP + FN)} \tag{22}$$

here True Positives (TP) are cases of the observed class that were correctly classified, False Positives (FP) are cases in other classes that are misclassified, True Negatives (TN) are the instances of the

remaining classes that are correctly classified, In the class under observation, False Negatives (FN) represents the number of instances that were misclassified and N is the total number of images.

Table No. 1
Efficacy evaluation of the proposed LichenNet for classification

Classes	Accuracy	Precision	Sensitivity	Specificity	F1 score
Fruticose	99.2	97.2	97.4	96.5	98.4
Crustose	99.3	98.3	96.7	97.2	97.1
Foliose	99.1	96.4	96.5	97.5	96.2

The effectiveness reached by the proposed model for classifying various lichen classes of lichen such as Fruticose, Crustose, and Foliose is exhibited in Table No. 1. The proposed LichenNet achieves the accuracy of 99.26% for gathered images from the

Western Ghats. Furthermore, the proposed LichenNet acquires the overall pre, spec, sen, and f1 of 97.03%, 96.86%, 97.06% and 97.23% respectively. The visual performance analysis of the proposed LichenNet is exposed in Figure No. 4.

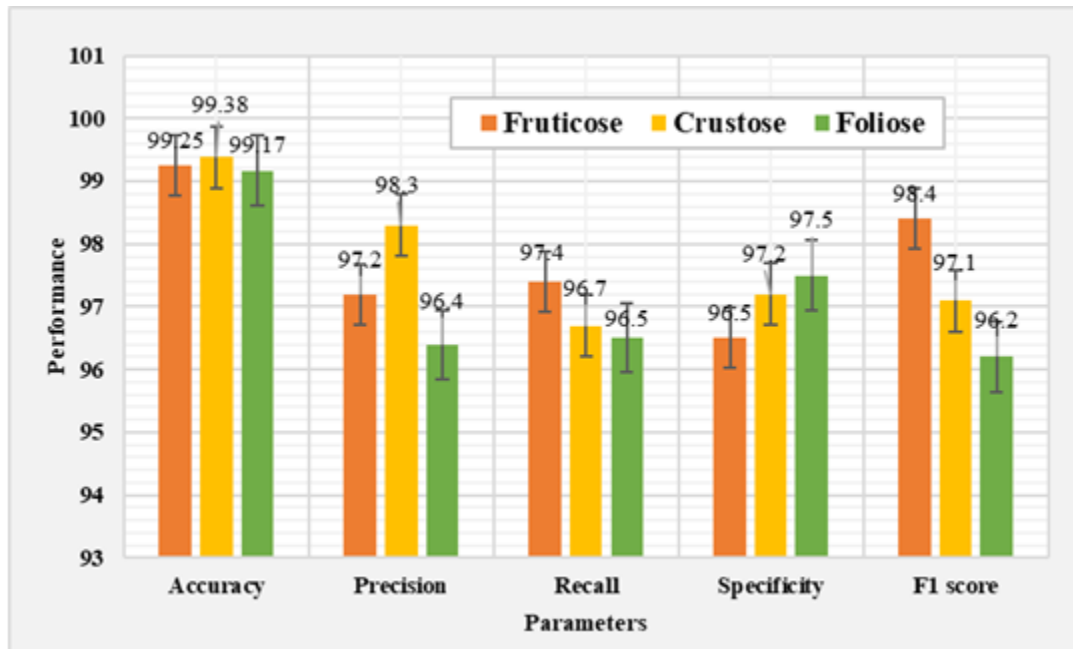


Figure No. 4
Visual competence evaluation of the proposed LichenNet

The proposed LinkNet was trained during 50 epochs with exactly the same configuration to attain best results. The graphs for the training and validation

sets of the collected datasets are displayed in Figure No. 6, where the three networks that are tested and plotted along with their accuracy and loss functions.



Figure No. 6
Loss curve of the proposed LinkNet

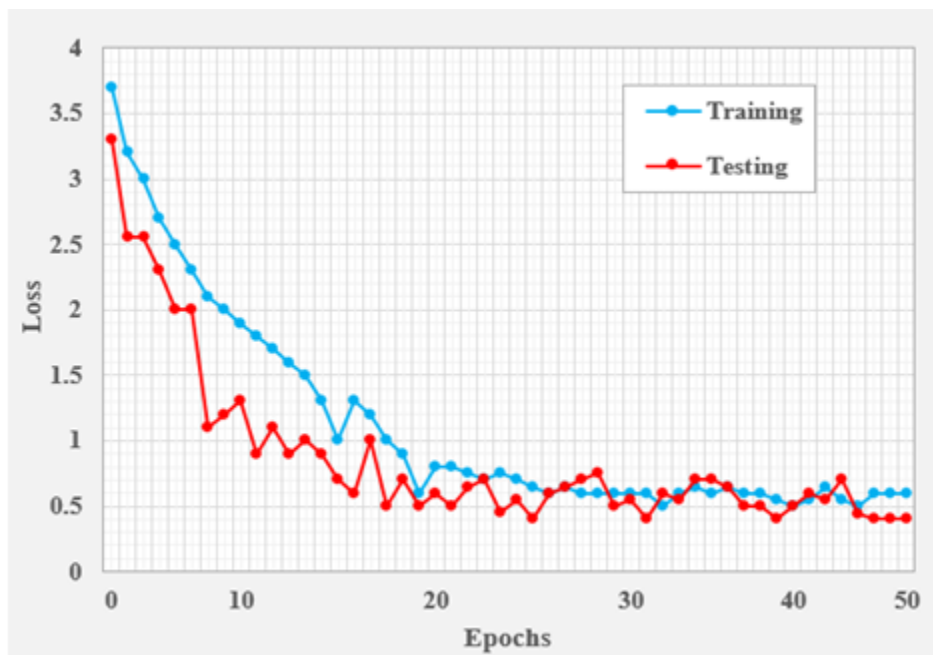


Figure No. 6
Loss curve of the proposed LinkNet

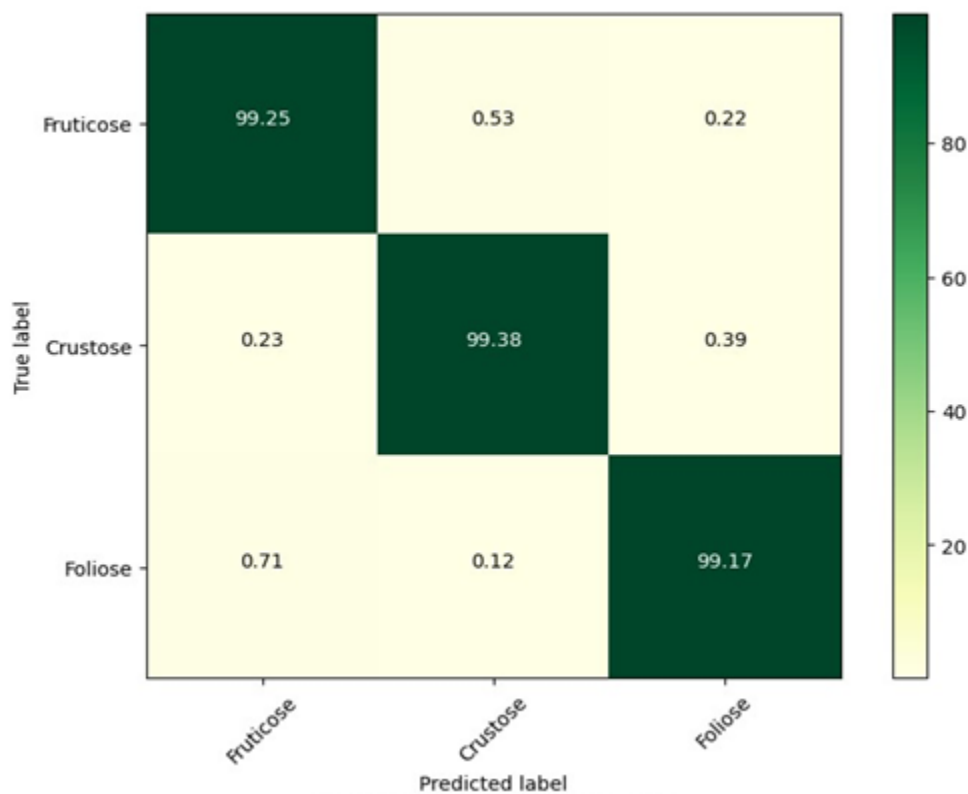


Figure No. 7
Confusion matrix for lichen classification

Figure No. 7 shows the 3x3 confusion matrix for classifying lichen types that representing the actual and predicted classes, respectively. Each cell counts the number of cases detected into a specific combination of classes. In this context, it could represent three different types of lichen (e.g., foliose, fruticose, crustose) with an overall accuracy of 0.9927 and loss of 0.0073. The diagonal elements specify precise categorization, while off-diagonal elements signify mis categorization. From this Figure No. 7, the efficiency of the proposed LichenNet attains best classification results.

Comparative scrutiny

The performance of each neural network was measured for validating the efficacy of the proposed approach in achieving highly accurate outcomes. Comparative evaluations were carried out between the proposed LinkNet and several other DL classifiers like DenseNet, AlexNet, and GoogleNet. Various parameters, including acc, pre, spec, sen, and F1 were employed to gauge efficiency across each network. Notably, the accuracy of the proposed LinkNet reached an impressive 99.26%, surpassing that of conventional deep learning networks.

Table No. 2
Comparison between the traditional DL networks for classification

Networks	Accuracy	Precision	Sensitivity	Specificity	F1 score
AlexNet	90.09	93.27	89.18	93.58	93.25
DenseNet	91.21	89.18	92.87	89.25	89.37
GoogleNet	89.90	92.76	90.39	92.78	91.91
LinkNet	99.26	97.03	97.06	96.86	97.23

From Table No. 2 we can compare several DL structures on the basis of their efficiency measures for determining the proper proportion of accuracy in classification. In comparison with the LinkNet,

conventional networks performed worse than LinkNet. The proposed LinkNet progresses the overall accuracy range by 9.24%, 8.11%, and 9.42% better than AlexNet, DenseNet and GoogleNet respectively.

Table No. 3
Accuracy comparison of the proposed model with the existing models

Authors	Method	Accuracy
Sandino <i>et al.</i> , 2023	XGBoost	97.08%
Presta <i>et al.</i> , 2022	SIFT	95.0%
Galanty <i>et al.</i> , 2021	CNN	85.0%
Proposed	Deep Lichen Net	99.26%

Table No. 3 illustrates the experimental duration of a sample input signal was calculated from the gathered dataset in order to verify the precision of different approaches. In order to compare earlier methods, particular performance indicators were used to ensure classification accuracy. The proposed LichenNet progresses the overall accuracy of 2.19%, 4.29%, and 14.36% for XGBoost (Mishra *et al.*, 2021), SIFT (Richardson *et al.*, 2023), and CNN (Lovitt *et al.*, 2022), respectively. Though, the prior methods did not attain good accuracy level compared to the proposed LichenNet.

for XGBoost, SIFT, and CNN respectively. The evaluation results establish the efficiency of the proposed technique in accurately identifying lichen species, achieving high classification accuracy rates. This approach offers a promising field for expediting lichen identification processes, facilitating ecological research, conservation efforts, and environmental monitoring. Future work could explore the integration of multispectral imaging techniques to enhance lichen classification accuracy and extend the application of the proposed LichenNet framework to diverse geographical regions for broader ecological insights.

CONCLUSION

This paper presents a novel Deep Lichen Net for classifying different lichen types in the Western Ghats using a gathered lichen dataset. The approach involves deep learning-based ROI patch extraction, dividing images into non-overlapping patches for feature extraction. LinkNet distinguishes between lichen species based on LoGo features, which are then optimized using the PeO algorithm for accurate classification into fruticose, crustose, and foliose taxa. The proposed LinkNet increases the overall accuracy range by 9.24%, 8.11%, and 9.42% better than AlexNet, DenseNet and GoogleNet respectively. Moreover, the proposed Deep LichenNet increases the overall accuracy of 2.19%, 4.29%, 14.36% and 6.88%

Competing interests

This paper has no conflict of interest for publishing

Informed consent

I certify that I have explained the nature and purpose of this study to the above-named individual, and I have discussed the potential benefits of this study participation. We will always be available to answer any questions that research reviewers may have in the future regarding this study.

ACKNOWLEDGMENTS

The author would like to express his heartfelt gratitude to the supervisor for his guidance and unwavering support during this research for his guidance and support

REFERENCES

- Dakshina DS, Della Reasa Valiaveetil, Bindhu A. 2023. Alzheimer disease detection via deep learning-based shuffle network. **Int J Curr Bio-Med Eng** 1: 9 - 15.
- Devaprakash M, Thirumalaivasan R, Sivakumar N, Shyamkumar R. 2024. Cyanobacterial interactions and symbiosis. **Cyanobacteria** 425 - 489. <https://doi.org/10.1016/B978-0-443-13231-5.00004-0>
- Dinesh JSR, Fenil E, Manogaran G, Vivekananda GN, Thanjaivadivel T, Jeeva S, Ahilan AJCN. 2019. Real time violence detection framework for football stadium comprising of big data analysis and deep learning through bidirectional LSTM. **Comp Net** 151: 191 - 200. <https://doi.org/10.1016/j.comnet.2019.01.028>
- Erlandsson R, Bjerke JW, Finne EA, Myneni RB, Piao S, Wang X, Virtanen T, Räsänen A, Kumpula T, Kolari TH, Tahvanainen T. 2022. An artificial intelligence approach to remotely assess pale lichen biomass. **Remote Sensing Environ** 280: 113201. <https://doi.org/10.1016/j.rse.2022.113201>
- Galanty A, Danel T, Węgrzyn M, Podolak I, Podolak I. 2021. Deep convolutional neural network for preliminary in-field classification of lichen species. **Biosyst Eng** 204: 15 - 25. <https://doi.org/10.1016/j.biosystemseng.2021.01.004>
- Granlund L, Keski-Saari S, Kumpula T, Oksanen E, Keinänen M. 2018. Imaging lichen water content with visible to mid-wave infrared (400 - 5500 nm) spectroscopy. **Remote Sensing Environ** 216: 301 - 310. <https://doi.org/10.1016/j.rse.2018.06.041>
- Guedes P, Oliveira MA, Branquinho C, Silva JN. 2022. Image analysis for automatic measurement of crustose lichens. **arXiv preprint arXiv: 2203.00787**. <https://doi.org/10.48550/arXiv.2203.00787>
- Haridas B, Aliyarukunju S, Sugathan S. 2023. **Lichen flora in Western Ghats of Kerala, India: A source of innovation**. In: Microbial biodiversity, biotechnology and ecosystem sustainability. Springer Nature Singapore, Singapore. https://doi.org/10.1007/978-981-19-4336-2_7
- Hrdina A, Romportl D. 2024. Global environmental systems: A spatial framework for better understanding the changing world. **Environments** 11: 33. <https://doi.org/10.3390/environments11020033>
- Idrees M, Farah CS, Shearston K, Kujan O. 2021. A machine-learning algorithm for the reliable identification of oral lichen planus. **J Oral Pathol Med** 50: 946 - 953. <https://doi.org/10.1111/jop.13226>
- Jozdani S, Chen D, Chen W, Leblanc SG, Lovitt J, He L, Fraser RH, Johnson BA. 2021. Evaluating image normalization via GANs for environmental mapping: A case study of lichen mapping using high-resolution satellite imagery. **Remote Sensing** 13: 5035. <https://doi.org/10.3390/rs13245035>
- Jung P, Briegel-Williams L, Werner L, Jost E, Schultz M, Nürnberg DJ, Grube M, Lakatos M. 2024. A direct PCR approach with low-biomass insert opens new horizons for molecular sciences on cryptogam communities. **Appl Environ Microbiol** 90: e0002424. <https://doi.org/10.1128/aem.00024-24>
- Kapoor L, Simkin AJ, Doss CGP, Siva R. 2022. Fruit ripening: dynamics and integrated analysis of carotenoids and anthocyanins. **BMC Plant Biol** 22: 1 - 22. <https://doi.org/10.1186/s12870-021-03411-w>
- Li Z, Zhu H, Huang M. 2021. A deep learning-based fine crack segmentation network on full-scale steel bridge images with complicated backgrounds. **IEEE Access** 9: 114989 - 114997. <https://doi.org/10.1109/ACCESS.2021.3105279>
- Lie MH, Arup U, Grytnes JA, Ohlson M. 2009. The importance of host tree age, size and growth rate as determinants of epiphytic lichen diversity in boreal spruce forests. **Biodiv Conserv** 18: 3579 - 3596. <https://doi.org/10.1007/s10531-009-9661-z>
- Lovitt J, Richardson G, Rajaratnam K, Chen W, Leblanc SG, He L, Nielsen SE, Hillman A, Schmelzer I, Arsenault A. 2022. A new U-Net based convolutional neural network for estimating caribou lichen ground cover from field-level RGB images. **Can J Remote Sensing** 48: 849 - 872. <https://doi.org/10.1080/07038992.2022.2144179>
- Malik OA, Puasa I, Lai DTC. 2022. Segmentation for multi-rock types on digital outcrop photographs using deep learning techniques. **Sensors** 22: 8086. <https://doi.org/10.3390/s22218086>
- Mishra GK, Maurya P, Bhatiya A, Upreti DK. 2021. *Mangifera indica* L. as an excellent host tree for colonization of tropical lichens in India. **Cryptogam Biodiv Assess** 5: 15 - 23.
- Ovstedal DO, Smith RL. 2001. **Lichens of Antarctica and South Georgia: A guide to their identification and**

- ecology**. Cambridge University Press, Cambridge, UK.
- Peng C, Li Y, Jiao L, Shang R. 2020. Efficient convolutional neural architecture search for remote sensing image scene classification. **IEEE Trans Geosci Remote Sensing** 59: 6092 - 6105.
<https://doi.org/10.1109/TGRS.2020.3020424>
- Prasanth A, Muthukumaran N. 2023. Primary open-angle glaucoma severity prediction using deep learning technique. **Int J Curr Bio-Med Eng** 1: 30 - 37.
- Preethaa KS. 2021. Lichen element based autonomous air pollution monitoring around smart cities: A deep learning approach. **Turkish J Comp Math Educ** 12: 151 - 161.
- Presta A, Pellegrino FA, Martellos S. 2022. Learning-based automatic classification of lichens from images. **Biosyst Eng** 213: 119 - 132. <https://doi.org/10.1016/j.biosystemseng.2021.11.023>
- Rajaprabu N, Ponmurugan P. 2022. Phorophyte specificity of lichen community, with ecological taxation in Suruli watershed, Southern Western Ghats. **Asian J Conserv Biol** 11: 66 - 76.
<https://doi.org/10.53562/ajcb.69756>
- Rehush N, Abegg M, Waser LT, Brändli UB. 2018. Identifying tree-related microhabitats in TLS point clouds using machine learning. **Remote Sensing** 10: 1735. <https://doi.org/10.3390/rs10111735>
- Richardson G, Knudby A, Chen W, Sawada, Lovitt J, He L, Naeni LY. 2023. Dense neural network outperforms other machine learning models for scaling-up lichen cover maps in Eastern Canada. **Plos One** 18: e0292839. <https://doi.org/10.1371/journal.pone.0292839>
- Sandino J, Bollard B, Doshi A, Randall K, Barthelemy J, Robinson SA, Gonzalez F. 2023. A green fingerprint of Antarctica: Drones, hyperspectral imaging, and machine learning for moss and lichen classification. **Remote Sensing** 15: 5658. <https://doi.org/10.3390/rs15245658>
- Spribile T, Tuovinen V, Resl P, Vanderpool D, Wolinski H, Aime MC, Schneider K, Stabentheiner E, Toome-Heller M, Thor G, Mayrhofer H, Johannesson H, McCutcheon JP. 2016. Basidiomycete yeasts in the cortex of ascomycete macrolichens. **Science** 353: 488 - 492. <https://doi.org/10.1126/science.aaf8287>
- Subbaiyan R, Ganesan A, Dhanuskodi S. 2023. Ecolichenology of Eastern Ghats diversity against climatic fluctuations in Kolli Hills, India. **Biodiversitas J Biol Divers** 24: 625 - 635.
<https://doi.org/10.13057/biodiv/d240171>
- Surendiran R, Thangamani M, Narmatha C, Iswarya M. 2022. Effective autism spectrum disorder prediction to improve the clinical traits using machine learning techniques. **Int J Eng Trends Technol** 70: 343 - 359.
<https://doi.org/10.14445/22315381/IJETT-V70I4P230>
- Vinayaka KS, Krishnamurthy YL. 2010. Ecology and distribution of lichens in Bhadra Wildlife Sanctuary, Central Western Ghats, Karnataka, India. **Bioremed Biodiv Bioavail** 5: 68 - 72.
- Vinayaka KS, Chetan HC, Mesta AR. 2016. Diversity and distribution pattern of lichens in the mid elevation wet evergreen forest, Southern Western Ghats, India. **Int J Res Stud Biosci** 4: 15 - 20.
- Wang Y, Jia S. 2024. MADRAS-NET: A deep learning approach for detecting and classifying android malware using Linknet. **Measurement: Sensors** 33: 101113. <https://doi.org/10.1016/j.measen.2024.101113>